

CHAPERONIN-MEDIATED PROTEIN FOLDING

D. Thirumalai and George H. Lorimer

*Center for Biomolecular Structure and Organization, Department of Chemistry and
Biochemistry, University of Maryland, College Park, Maryland 20742;
e-mail: dt5@umail.umd.edu, GL48@umail.umd.edu*

Key Words GroEL, GroES, iterative annealing, nested cooperativity, protein machines

■ **Abstract** Molecular chaperones are required to assist folding of a subset of proteins in *Escherichia coli*. We describe a conceptual framework for understanding how the GroEL-GroES system assists misfolded proteins to reach their native states. The architecture of GroEL consists of double toroids stacked back-to-back. However, most of the fundamentals of the GroEL action can be described in terms of the single ring. A key idea in our framework is that, with coordinated ATP hydrolysis and GroES binding, GroEL participates actively by repeatedly unfolding the substrate protein (SP), provided that it is trapped in one of the misfolded states. We conjecture that the unfolding of SP becomes possible because a stretching force is transmitted to the SP when the GroEL particle undergoes allosteric transitions. Force-induced unfolding of the SP puts it on a higher free-energy point in the multidimensional energy landscape from which the SP can either reach the native conformation with some probability or be trapped in one of the competing basins of attraction (i.e., the SP undergoes kinetic partitioning). The model shows, in a natural way, that the time scales in the dynamics of the allosteric transitions are intimately coupled to folding rates of the SP. Several scenarios for chaperonin-assisted folding emerge depending on the interplay of the time scales governing the cycle. Further refinement of this framework may be necessary because single molecule experiments indicate that there is a great dispersion in the time scales governing the dynamics of the chaperonin cycle.

CONTENTS

PURPOSE	246
INTRODUCTION	246
THE CHAPERONIN HEMICYCLE	247
GroEL Heptamer as the Fundamental Unit	247
Capture	247
Encapsulation	253
ATP Hydrolysis and Ring Conditioning	255
Ligand Release and Domain Relaxation	256
ITERATIVE ANNEALING MECHANISM	257
Kinetic Partitioning Mechanism	257
Theoretical Considerations	259

COMMUNICATION BETWEEN RINGS	260
Allosteric Transitions	260
Allosteric Transitions and SP Folding	262
SINGLE MOLECULE MEASUREMENTS	263

PURPOSE

Our goal is to describe the mechanisms of chaperonin-mediated protein folding. The viewpoint described brings together concepts proposed in studies of unassisted folding and the unfolding of globular proteins. The resulting synthesis gives a coherent picture of how this remarkable machine dynamically interacts with a variety of structurally unrelated proteins in their misfolded states, thus enabling them to reach the native state.

Machine, *n*: a device that transmits or modifies force or motion. Webster's College Dictionary 2000.

INTRODUCTION

The last decade has witnessed several developments with respect to our understanding of protein folding. A development of a more biological nature was the realization that protein folding *in vivo* is not always an entirely spontaneous event. Instead, there are a group of proteins, collectively termed molecular chaperones (49), that, driven ultimately by the hydrolysis of ATP, facilitate the folding of some other proteins (16, 45). Of all molecular chaperones, the chaperonin proteins GroEL and GroES are the best understood, both structurally and mechanistically. It is easier to decipher mechanisms if the structures along the reaction pathways are known. The determination of the structures associated with the chaperonin system (4, 68) has sharpened our understanding of GroEL function. No point would be served rehashing the structural details that have already been the subject of two excellent reviews (53, 69).

Development of a coherent picture of GroEL-assisted folding requires incorporation of several developments that have contributed to our understanding of how a monomeric globular protein folds. First, that significant folding events occur on the time scale of 10^{-8} to 10^{-4} sec is now much more widely appreciated (11), and studies are now under way to explore these early folding events (37, 51). Second, single molecule "stretching" experiments that use optical tweezers and atomic force microscopy have convincingly demonstrated that it is possible to unfold proteins and other biopolymers by subjecting them to mechanical stress (20). Third, theoreticians familiar with many aspects of polymer physics have brought statistical mechanics to bear on the folding of biopolymers (10, 41, 56); from this, the concepts of energy landscapes have emerged. These ideas have been applied to shed light on the way chaperonins function (5, 24, 54). Our goal here is to present a view of the chaperonins that incorporates many of the developments alluded to above.

Before considering the individual steps of the complete chaperonin cycle, some remarks about the SP are in order. First, the vast majority of studies on chaperonins

have employed biologically heterologous combinations, most often chaperonins from *Escherichia coli* (GroEL/GroES) and SPs from just about every other organism but *E. coli*. Although a number of different *E. coli* proteins interact with GroEL in vitro (8, 12, 19), no *E. coli* protein has been identified whose in vitro folding is absolutely dependent upon GroEL. On the contrary, all of the commonly used SPs for GroEL can be induced to fold spontaneously, provided that a modest effort is expended to find the appropriate conditions. Nevertheless, it is useful to distinguish between permissive and nonpermissive conditions. Under permissive conditions, spontaneous folding to the native state occurs in vitro on a biologically relevant time scale. (For *E. coli* proteins at 37°C, that is maximally between 20–40 minutes, the doubling time of the cell.) Under nonpermissive conditions, spontaneous folding does not occur in vitro on a biologically relevant time scale. Under such conditions, barriers of sufficient magnitude separate the non-native states from the native state. This may be the consequence of aggregation, the formation of non-native, domain-swapped oligomers, or it may be attributed to the formation of kinetically trapped monomers or misfolds. From a biological standpoint, the most remarkable feature of the complete chaperonin system (GroEL, GroES, and MgATP) is its ability to permit the in vitro folding of SPs to their native states under otherwise nonpermissive conditions. Note that the complete chaperonin system enhances the yield of native SP (15, 57). Only rarely is the rate of formation of the native state enhanced by the chaperonins. More often the rate is unaffected or even decreased.

THE CHAPERONIN HEMICYCLE

GroEL Heptamer as the Fundamental Unit

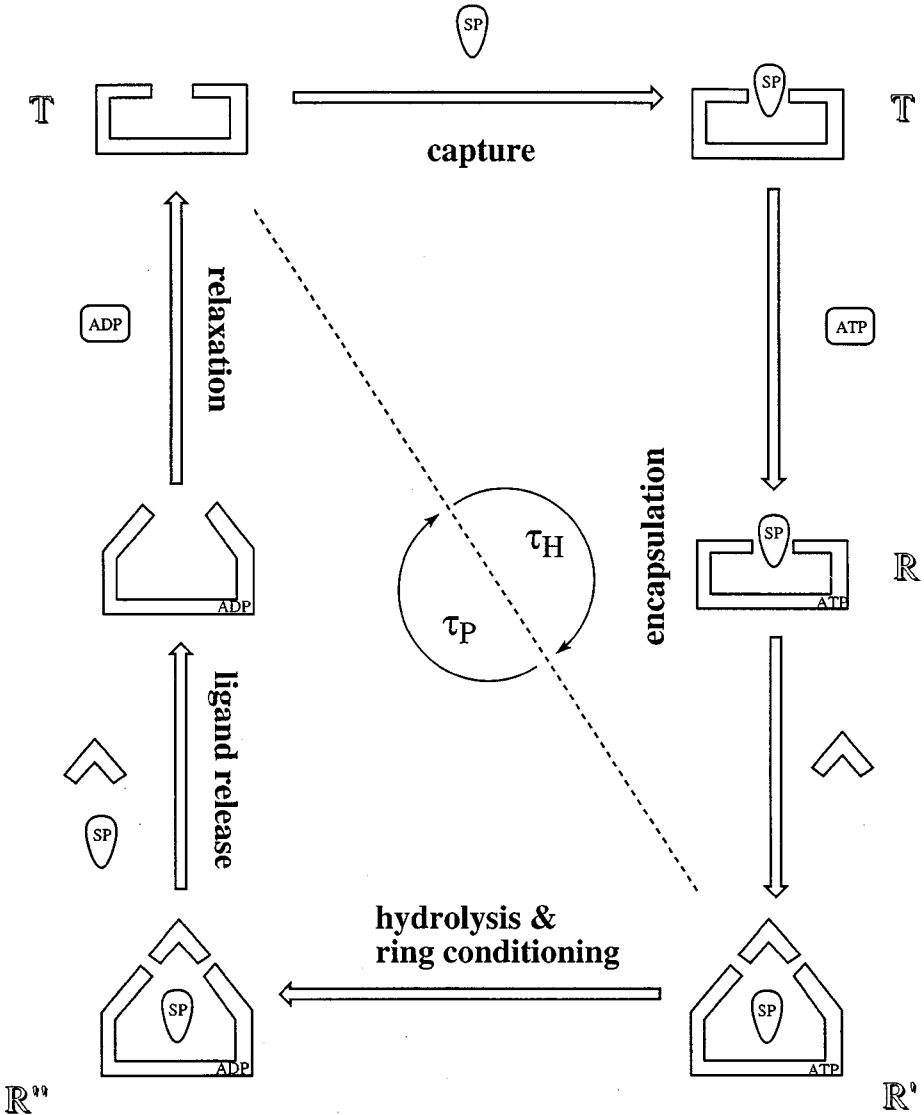
The most common form of the class I chaperonins consists of two heptameric rings, stacked back-to-back, that communicate with one another and that operate in a coordinated manner (33, 69). Although most of the experimental data have been gathered with studies of the double rings, from the standpoint of assisted protein folding, the single ring constitutes the fundamental unit. We therefore discuss the operation of the single ring, postponing until later a consideration of the manner in which the rings communicate with one another.

We start by considering the states through which the single ring progresses in the course of a hemicycle. The hemicycle can be broken down into a series of four sequential events (Figure 1) that we describe below. The total cycle time of a single ring is about 15 s at 37°C. The lifetime of all the individual states is currently unknown, although single molecule experiments have been initiated (60), which should help define the longevity and dispersion of the states.

Capture

The ability of GroEL to interact with a wide variety of proteins that, in their native states, bear little structural resemblance to one another could be discerned

from early genetic experiments. Many temperature-sensitive mutations in structurally unrelated proteins can be suppressed in vivo by overexpressing both GroEL and GroES in *E. coli* (14, 21, 59). In vitro studies confirmed this promiscuous behavior. Almost 50% of the soluble proteins of *E. coli* are able to form a stable binary complex with GroEL in vitro, provided they are presented to the chaperonin in a denatured state (61). These results clearly exclude a sequence-based



recognition motif. In general, GroEL does not interact with native proteins. Consequently, the structural element responsible for the interaction must be missing from, or more probably, inaccessible in, the native protein.

This conclusion is supported by the recent observation that GroEL binds artificial proteins (1). A set of seven proteins, each about 140 residues in length and each containing a unique but randomly chosen amino acid sequence with no propensity to fold to a unique native-like state, was biosynthesized. After purification, all seven artificial proteins bound to GroEL. Thus, GroEL apparently shows no preference for any particular secondary structure. This contradicts the assertion that GroEL interacts preferentially with α/β proteins (27).

However, marginally stable native proteins, particularly those that are monomeric, can form stable binary complexes with GroEL. In such instances, the native state exists in equilibrium with non-native conformers; and the favorable free

←

Figure 1 The chaperonin hemicycle. Although GroEL consists of two heptameric rings that operate in a coordinated manner (33), from the standpoint of chaperonin-assisted protein folding, the single ring represents the fundamental unit. The chaperonin hemicycle consists of several steps. Capture: In this stage the SP, generally in a non-native conformation, is captured and bound cooperatively by some (not necessarily all) of the seven predominantly hydrophobic peptide binding sites that are part of the apical domain and line the mouth of the GroEL cavity. SP binds preferentially to the *T* state. Encapsulation: This stage constitutes the “power stroke” of the cycle and occurs in two stages. It is initiated by the binding of ATP to the equatorial domain of GroEL, which induces a concerted $T \longleftrightarrow R$ transition. GroES binds exclusively to the apical domain of the *R* state. Large, entirely concerted, rigid-body domain movements occur, pivoting around the two hinges at the junctions between the equatorial, intermediate, and apical domains. These movements ultimately result in the vectoral displacement of SP into the central cavity of GroEL. Several important events occur during encapsulation. First, the ATP binding site is closed, and the ATP becomes committed to hydrolysis. Second, the concerted movement of the domains doubles the volume of the central cavity. Adjacent peptide binding sites, initially 25 Å apart center-to-center, are dispersed, ending up 33 Å from one another. Additionally, the surface of the central cavity changes from being predominantly hydrophobic to being largely hydrophilic and will remain so until relaxation completes the cycle and restores the hydrophobic surface associated with the capture complex. The time during which SP experiences a hydrophobic surface is approximated as τ_H , whereas the time SP experiences a hydrophilic surface is approximated as τ_P . The encapsulated $GroEL_7 \bullet ATP_7 \bullet SP \bullet GroES_7$ adopts the *R'* state. ATP hydrolysis and ring conditioning: In the encapsulated complex the ATP is committed to hydrolysis, which conditions the ring for subsequent steps. We designate the conditioned product complex $GroEL_7 \bullet ADP_7 \bullet SP \bullet GroES_7$ as the *R''* state. ATP hydrolysis serves as a timing device, specifying the lifetime of the encapsulated state. Ligand discharge: Binding of ATP to the distal ring initiates the dissociation of the conditioned product complex $GroEL_7 \bullet ADP_7 \bullet SP \bullet GroES_7$. After dissociation of the “keystone” GroES, SP diffuses out of the expanded central cavity, permitting relaxation to the capture complex. Relaxation involves a reversal of the concerted rigid-body domain movements that occurred during encapsulation. The central cavity contracts in volume, the hydrophobic peptide binding sites in the apical domain are restored, the nucleotide binding site is unlocked, and the product ADP is permitted to dissociate, regenerating the starting *T* state. See text for details.

energy of binding of GroEL to these non-native conformer(s) offsets the unfavorable free energy of unfolding of the native state to the non-native conformer(s) (8, 63).

The structural feature common to most non-native conformers is an exposed hydrophobic surface that very often becomes buried during the transition to the native state. Calorimetric (31) [but see also (2)], enzymatic (46), and structural analyses (7) confirm that hydrophobic interactions constitute a major, although not the sole, determinant governing the interaction between GroEL and its SPs. Electrostatic interactions also contribute (7, 29, 43, 44).

The site of SP binding was first defined by mutational analyses (6, 7, 17). When mapped onto the crystal structure of GroEL, the mutants that were defective in binding SP clustered in the apical domain, more specifically in the groove between helices H and I and in the adjacent region including the bulky hydrophobic residues Y203, F204, and L259. More detailed crystallographic analyses of the binding of peptides to the groove between helices H and I have been published (6, 7). Some caution should be exercised here, for the region between helices H and I is destined to become the very region occupied by the so-called mobile loops of GroES. Are the peptides found in the respective crystal structures genuine surrogates for SP, or are they merely mimics of the mobile loop of GroES? Perhaps they are both.

In any event, these two adjacent hydrophobic regions are repeated sevenfold so that the inner surface of the ring of apical domains presents a more or less continuous hydrophobic surface, upon which the exposed hydrophobic surfaces of the non-native SPs become ensnared. Any given SP, most likely an ensemble of non-native conformational states, may thus be bound cooperatively at from 1 to 7 sites. Because different regions of the SP may contact GroEL at different sites, the binding thermodynamics likely vary from site to site. In addition, the total number of sites that engage the SP likely varies from one individual complex to the next. Some GroEL-SP complexes may involve binding at 3 sites, some at 4 sites, and so on. Considerable dispersion and nonergodic behavior is therefore expected in the energetics of SP binding. A recent atomic force microscopy (AFM) study (62) measuring the force required to disrupt binary complexes of T-state GroEL and non-native citrate synthase provides experimental evidence for this.

The number of GroEL sites that engage the SP has recently been addressed with a remarkable genetic construct of GroEL, a fused 7-mer constructed by linking, head-to-tail, seven copies of the *groEL* gene (13). The fused 7-mer, a polypeptide of some 420 kilodalton, nevertheless folds and assembles into the familiar seven-membered rings stacked back-to-back. This permitted the introduction of mutant binding sites at specific positions in multiples from 0–7, including positional variants. Although the SP binding assay was qualitative [the ability of binary complexes of mutant GroEL•SP to survive passage through an analytical gel filtration column (passage time about 7 min)], several insights were achieved. Using the above criterion, not all seven wild-type binding sites were necessary. Indeed, as many as 3–4 mutant sites could be introduced into the 7-mer before a decrease in recovery of the GroEL-SP complex was detected. A quantitative study, specifically using AFM to determine both the mean force needed to disrupt these

various mutant binary complexes and the dispersion of force would be particularly insightful. We would expect the mean force and the dispersion of force to diminish as the number of mutant sites in the ring increased.

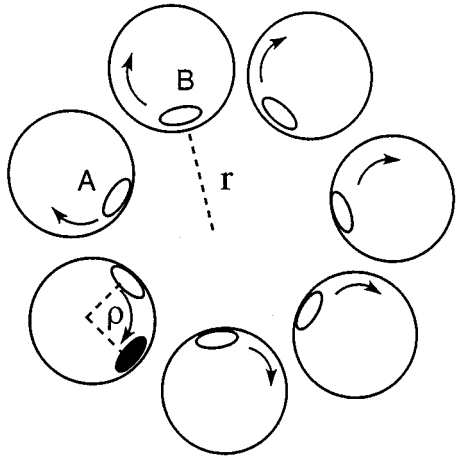
The volume of the GroEL cavity in the *T* state (that which binds SP most tightly) is $85,000 \text{ \AA}^3$ (69). The diameter of the pore surrounding the sevenfold axis of symmetry is about 45 \AA . This limits access to the entire cavity to proteins smaller than about 30 KDa. However, much larger proteins, even those exceeding 100 KDa in size, can form stable binary complexes with GroEL. In such instances, it is clear that a substantial part of the SP must reside outside the cavity, even as other parts are bound within.

A major factor influencing the binding of various SPs to GroEL concerns the conformational state of the latter, *T* or *R*. The *T* state has the greater affinity for SP. The transition to the *R* state is induced by the binding of ATP (70). The *R* state thus has a greater affinity for ATP than the *T* state. The $T \longleftrightarrow R$ transition is entirely concerted in nature (35, 69). A model of nested cooperativity (71) in which the $T \longleftrightarrow R$ transition within a ring is described by the Monod-Wyman-Changeaux (MWC) (36) treatment—an all or none model—satisfactorily describes the steady state and presteady state kinetics of ATP hydrolysis (26, 71). In addition, structural considerations (69) as well as molecular dynamic simulations (34, 35) point to a concerted $T \longleftrightarrow R$ transition. Finally, cross-linking studies demonstrate that the introduction of a single interdomain tether is sufficient to lock the entire ensemble of seven subunits in the *T* state (G Curien & GH Lorimer, unpublished data).

The binding of SP to GroEL also locks the ring in the *T* state (70). The latter observation is particularly interesting in light of the structural changes that accompany the $T \longleftrightarrow R$ transition. Cryo-electron microscopy (Cryo-EM) of GroEL•ATP complexes (i.e., *R* state complexes) shows that in undergoing the concerted $T \longleftrightarrow R$ transition each apical domain twists in a clockwise direction with respect to the equatorial domain (66). Simple geometric considerations (Figure 2) show that this transition will be accompanied by the moving apart of the SP binding sites, nonadjacent sites moving further apart than adjacent sites. The binding of SP stimulates the ATPase activity. This phenomenon can be attributed to the fact that the activity (k_{cat}) of a subunit in the *T* state is 4–5 times greater than the activity of a subunit in the *R* state. That indicates that SP resists the $T \longleftrightarrow R$ state transition (70). A corollary of this statement is, in proceeding from the *T* to the *R* state, force is exerted on the SP (52). This also follows from the fact that SP binding sites move apart from one another in the $T \longleftrightarrow R$ transition (Figure 2). Provided that the binding of the SP to the various sites is sufficiently strong, the force on the SP can unfold its higher order (secondary and tertiary) structural elements. This is analogous to forced-induced unfolding of proteins observed by AFM or optical tweezers (20).

Cryo-EM studies (66) suggest that the twisting movement accompanying the $T \longleftrightarrow R$ transition causes at least part of the bipartite SP binding site to become sequestered in a new subunit-subunit interface. It is further known that the binding of SP to GroEL is significantly weakened upon binding ATP (70), that is upon $T \longleftrightarrow R$ transition. This is reflected in the results of AFM force measurements

distance $AB = 2\pi r / \gamma$

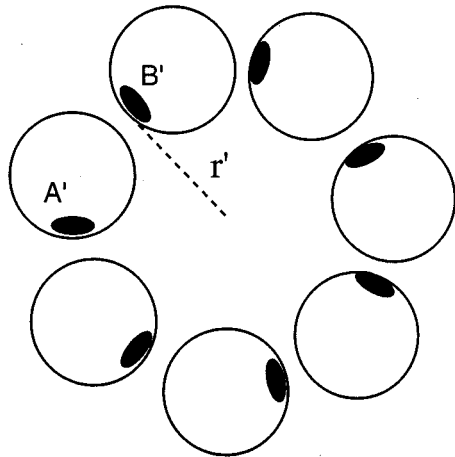


T

ATP



distance $A'B' = 2\pi r' / \gamma$



R

when $r' > r$, $A'B' > AB$

performed in the presence of ATP (62). Not only is the mean force needed to disrupt the complex much reduced, but the dispersion of force is also diminished (62). This is attributed to a reduction in the number of sites binding the SP and/or to a reduction of the binding energy at each site.

Encapsulation

Encapsulation is the process whereby the SP becomes completely sequestered from the external environment within the central cavity of GroEL beneath the GroES cap. During encapsulation, the SP goes from a state in which it is bound on GroEL to one in which it is sequestered within the chaperonin. This is not a mere semantic distinction because it pertains to the nature of the interactions between SP and GroEL. In the former state, the SP is to some extent conformationally restrained by virtue of being bound on GroEL, whereas within the cavity the SP is, to a first approximation, conformationally unrestrained. The encapsulation is accompanied by several mechanistically significant events and can be considered as the power stroke of the chaperonin cycle. The binding of MgATP to the active site in the equatorial domain triggers a series of concerted, rigid-body, domain movements that are amplified in the presence of GroES (49, 53).

In response to the binding of ATP, each intermediate domain exercises a 25° en-bloc movement toward the equatorial domain around two hinges, Pro 137 and the absolutely conserved Gly410 (68, 69). This downward movement of the intermediate domain brings the carboxylate group of D398 of helix M into the inner coordination sphere of the magnesium ion that is associated with the γ phosphoryl moiety of ATP. The carboxylate of D398 is essential for ATP hydrolysis. This collapse of the intermediate domain over the nucleotide binding site can occur independently of the $T \longleftrightarrow R$ transition, because both states can hydrolyze ATP (G Curien & GH Lorimer, unpublished data).

On the other hand, the binding of GroES depends upon the the $T \longleftrightarrow R$ transition, the concerted twisting of the apical domain relative to the equatorial domain. The docking of one or more of the mobile loops of GroES into the cleft between helices H and I triggers a more extensive movement of the apical domains, which move upward by 60° and complete a 90° twist with respect to the equatorial domains (53). The introduction of a single interdomain tether is sufficient to prevent this transition, indicating that the $R \longleftrightarrow R'$ transition is concerted

Figure 2 Dispersal of the SP binding sites during the $T \longleftrightarrow R$ transition. Cryo-electron microscopy (66) has revealed that the apical domain, containing the SP binding sites, undergoes a clockwise twisting motion relative to the equatorial plate upon binding of ATP (i.e., during the $T \longleftrightarrow R$ transition). Two SP binding sites, A and B, are shown initially in the T state. The distance AB, from one SP binding site A to an adjacent site B is given by $2\pi r/7$, where r is the internal radius of the ring. After twisting through ρ degrees, the SP binding sites are located at A' and B' , which are now located r' from the sevenfold axis of symmetry. When $r' > r$, it follows that the distance $A'B' > AB$ ($\Delta x = A'B' - AB$); the SP binding sites are more distant from one another in the R state than in the T state. See text for details.

(G Curien & GH Lorimer, unpublished data). This is borne out from structural (53) and molecular dynamics simulation studies (35).

The number of GroES mobile loops that interact with GroEL has recently been addressed with the fused 7-mer of GroEL. Mutations in the binding sites for the GroES mobile loops were introduced at specific positions in the fused 7-mer in multiples from 0–7, including positional variants. Although the GroES binding assay was qualitative, GroEL was able to accommodate as many as 5 mutant subunits in the heptameric ring without diminishing the yield of GroEL-GroES complex (13). As was the case with the binding of SP, not all seven GroES binding sites appear to be necessary. This finding resolves two related puzzles that arose when it was realized that the SP and the mobile loops of GroES shared a common binding site. How could GroES bind when the sites were already occupied by SP? How could GroES binding (encapsulation) result in the vectorial displacement of the SP into the expanded central cavity? It is now apparent that the SP need only be bound at a subset (say 3 or 4) of the 7 available sites, which leaves the remaining sites available for interaction with the mobile loops of GroES. When, as a result of the massive domain movement, the SP is displaced from its binding sites, its path to the bulk medium would be blocked by GroES, and vectorial displacement to the central cavity would be ensured. The sites that were initially occupied by SP can now be occupied by the remaining mobile loops of GroES.

The encapsulation process expands the volume of the central cavity approximately twofold, to about $170,000 \text{ \AA}^3$. This clearly sets an upper limit to the size of the SP that can be accommodated. Theoretical considerations of packing density, together with experiments with multimers of green fluorescent protein, place this upper limit at approximately 58,000 dalton (50). Assuming a spherical shape, a SP of this size would be expected to have a radius of about 30 \AA in its native state (67). Allowing that the “molten globule” state is slightly ($\sim 10\%$) larger yields a radius of 33 \AA . Treating the central cavity as a sphere yields a radius of about 35 \AA . For SPs approaching the upper size limit, there can only be a layer of one or two water molecules between the surface of the central cavity and the surface of the SP.

Amide tritium exchange experiments (52) are consistent with an unfolding event occurring during encapsulation. A small core of stable amide tritium atoms bound to Rubisco in a binary complex of GroEL•Rubisco was discharged within 4 sec (the resolving time of the experiment) after the addition of both ATP and GroES. Attempts to extend this result to other SPs have been unsuccessful; most lack the core of protected amide tritium upon which the above result with Rubisco depends. The results of fluorescence anisotropy measurements (48) are also consistent with the SP becoming less structured during the first second of the encapsulation process.

The polarity of the surface of the central cavity undergoes a dramatic change upon encapsulation (68, 69). Whereas the surface was predominantly hydrophobic in the *T* state, the surface becomes predominantly polar or hydrophilic in the encapsulated *R'* state. It remains in this state until the completion of the cycle, when the reverse domain movements return the system to the *T* state. This switching between hydrophilic and hydrophobic surfaces, as well as the duration of each state,

has profound implications on the microenvironment sensed by the SP. The consequence of this switch on the assisted folding mechanisms is discussed below. In addition to the altered surface properties that accompany the $R \longleftrightarrow R'$ transition, the concerted domain movement brings about a further dispersal of the peptide binding sites (33). In the resting T state, the peptide binding sites of adjacent subunits are 25 Å apart. Following encapsulation, the same peptide binding sites are 33 Å apart. There is, thus, an 8 Å differential between adjacent subunits and a maximal of 17.4 Å differential between nonadjacent subunits. The mechanical movement that accompanies encapsulation is likely to exert force on a SP spanning two such sites. The magnitude of the stretching force exerted on the SP during the $R \longleftrightarrow R'$ transition may be larger than in the initial $T \longleftrightarrow R$ transition. When the stretching force exceeds a threshold value determined by the interactions between the SP and GroEL, the SP will be released vectorially into the central cavity. The implication that work is performed on the SP during encapsulation clearly distinguishes this mechanism of chaperonin action from other more passive models. A testable corollary of this idea is that the presence of SP should slow the rate of the $R \longleftrightarrow R'$ transition.

Several SPs have been observed to fold to the native state (or, in the case of oligomeric proteins, to assembly-competent states) while encapsulated in the central cavity (22, 65). These studies generally involve artificially extending the lifetime of the encapsulated complex by using single-ringed mutants of GroEL that are unable to perform more than a single cycle. Such studies demonstrate unequivocally that folding to the native state can occur following encapsulation. The proponents of passive mechanisms point to such studies as evidence that merely sequestering the SP within the cavity is sufficient. In this view, no work is done on the SP. However, this overlooks the distinct possibility that during the very act of encapsulation work is indeed done on the SP.

An additional assumption, tacitly made by the proponents of passive mechanisms, concerns the stability of monomeric states, formed within the encapsulated complex, that are destined to oligomerize upon release. While many of these monomers may be both stable and assembly competent, this is clearly not always so. In the case of citrate synthase (22) and the β -subunit of bacterial luciferase (15), the assembly-competent monomer is a transient high-energy species that isomerizes to a more stable but assembly-incompetent form. Nevertheless, those stable assembly-incompetent forms can be rescued by GroEL and, in the presence of GroES and ATP, converted back to unstable assembly-competent forms. For such oligomeric proteins, the iterative annealing mechanism provides a means for regenerating transiently stable assembly-competent monomers.

ATP Hydrolysis and Ring Conditioning

An important consequence of encapsulation is the commitment to hydrolysis of the ATP that is locked into the active site (58). At ATP concentrations typically found in vivo, it is probable that all seven sites of the encapsulated complex are populated with ATP. Because all seven ATP are committed to hydrolysis, this gives rise to the

“quantized” nature of ATP hydrolysis in the presence of GroES (58). The hydrolysis of ATP serves as a timing device, controlling the lifetime of the encapsulated state. Single-molecule AFM measurements (60) indicate that the mean residence time of GroES on a GroEL ring is in the order of 7 sec, although considerable dispersion is evident. This mean residence time is not to be confused with the total cycle time. Presently we do not know what effect, if any, the presence or absence of an encapsulated SP might have on the residence time of GroES on GroEL. Only when ATP hydrolysis is complete is the ring conditioned for subsequent steps in the cycle (48). While inorganic phosphate is able to escape the active site, ADP remains locked in the active site (8a). In the normal course of events, the signal that destabilizes this product complex originates in the distal *trans* ring. Because they lack the distal ring, single-ring variants of GroEL become arrested at this point in the cycle. However, the single-ringed GroEL₇•ADP•GroES₇ complex can be destabilized by mutation (39, 40), which permits single rings to turn over and perform as efficiently as the double-ringed version.

The $R' \longleftrightarrow R''$ transition accompanies ATP hydrolysis and ring conditioning. From a structural standpoint, the only difference between the R' and R'' states may be the all important presence or absence, respectively, of the β, γ phosphoryl anhydride bond.

Ligand Release and Domain Relaxation

The binding of another molecule of SP to the distal *trans* ring only occurs after ATP hydrolysis in the *cis* ring (48). This may be a consequence of decreased cooperativity in the *trans* ring when GroES is bound to the *cis* ring (27a). However, the binding of SP to the distal *trans* ring is not sufficient, in and of itself, to induce ligand release from the *cis* ring (58). The release of all three ligands, GroES, SP, (folded or not), and ADP, from the *cis* ring is triggered by the binding of ATP to the distal ring (48, 58, 64). However, the rate of the ATP-dependent ligand release is accelerated 20–50-fold by the presence of SP on the distal ring (48). The binding of SP to the distal ring tends to stabilize the latter in the T state, and the observed enhancement in the rate of ligand release could be attributed to this. Nevertheless, cross-linking experiments that lock the distal ring in the T state indicate that inter-ring communication, which is triggered by the binding of ATP to the distal ring, does not depend upon that ring undergoing a $T \longleftrightarrow R$ transition (G Curien & GH Lorimer, unpublished data).

To a first approximation, the discharge of the ligands from the *cis* ring presumably occurs by a reversal of the steps occurring during encapsulation. The reaction is ordered with GroES leaving first, followed by SP. During this process, the volume of the central cavity contracts from 175,000 Å³ to 85,000 Å³, and the apical domain relaxes in a concerted manner from the R'' state via the R state to the T state. The hydrophobic surface of the central cavity is reestablished. The intermediate domain retracts, releasing the ADP from the active site. Especially for SPs, which are only just accommodated in the expanded cavity, it is clear

that the apical domains could not relax until after the SP has departed. Therefore that the release of ADP follows the relaxation of the apical domains. Because ATP hydrolysis in the other ring only occurs after ADP has been released, it follows that SP must be cleared from the cavity to ensure continued operation of the system. The release of the SP with each round of ATP hydrolysis has been repeatedly demonstrated (58, 64).

ITERATIVE ANNEALING MECHANISM

Using the individual steps in the fundamental cycle (Figure 1), we develop a quantitative description of the events leading to the rescue of SP. The outlines of this model (9, 57), which are derived from an energy landscape perspective, are based on the premise that GroEL plays an active role in enabling the SPs to fold. Several experiments suggest that as the GroEL particle undergoes allosteric transitions, it enables the SPs to unfold (38, 52, 74), supporting the idea of active GroEL participation in assisted folding. The model generalizes the theoretical description of monomeric folding of proteins (10, 41, 56) to include the role of chaperonins. The resulting iterative annealing mechanism (IAM) has been further refined to properly account for the participation of the second ring (47).

It is thought that a large fraction ($\approx 0.8-0.9$) of proteins in *E. coli* fold independently of chaperonins under normal cellular conditions (32). There is a small fraction whose free energy landscape under nonpermissive conditions consists of several competing basins of attractions (CBAs) in addition to the native basin of attraction (NBA). As described above, the CBAs could correspond to aggregates or misfolds. In either case, the CBAs serve as kinetic traps. If the traps are deep enough, as often appears to be the case for large proteins, spontaneous folding on biologically relevant time scale is unlikely. Chaperonins prevent aggregation and rescue misfolded proteins by utilizing the energy from coordinated ATP hydrolysis in a dynamic manner in which GroEL undergoes a series of large conformational changes (Figure 1) (54, 58, 64). Because the interaction between chaperonin and the SP is stochastic in nature, sufficient yield of the native state may require multiple rounds of encapsulation and release. The number of rounds of binding and release depends on several distinct time scales.

Kinetic Partitioning Mechanism

Before describing the basis of the IAM in detail, it is useful to understand the kinetic partitioning mechanism (KPM) by which a monomeric protein folds (25). The KPM follows from the analysis of the rugged free energy landscape of proteins (56). It is well accepted that the underlying energy landscape of proteins is rough, consisting of many minima that are separated by a distribution of barrier heights (10, 41, 56). For proteins that do not require chaperonins (those that fold spontaneously and within several milliseconds), the barriers are sufficiently small that they are readily overcome. These are typically “two-state” folders.

The energy landscape of such sequences is simple. They are presumed to be funnel-shaped (10, 41). For such proteins, all molecules reach the native state by a direct pathway involving a nucleation-collapse mechanism (18, 25). On the other hand, for certain proteins (especially larger proteins under nonpermissive conditions), there can be an ensemble of low-energy minima that require large activation energies to escape from the trapped states. The structures in the low-energy minima may have many aspects in common with the native structure, but they also contain non-native tertiary interactions. Thus, after an initial nonspecific collapse of the polypeptide chain, many of the molecules become trapped for arbitrarily long times in one of the low-energy minima (CBAs). Thus, generically we expect the free energy of a polypeptide chain to have a multivalley structure (41, 56).

Qualitative description of the kinetics leading to KPM follows from the underlying energy landscape. Imagine a process by which an ensemble of unfolded structures begins to navigate in the rough free energy landscape in search of the native conformation. A fraction of molecules, Φ , whose conformations map directly onto the NBA, would fold to the native state without encountering any discernible intermediates. The remaining fraction, $1 - \Phi$, would necessarily land in one of the CBAs. Because subsequent rearrangement requires activation over a free energy barrier, the folding of this set of molecules would be slow. Due to the multivalley structure of the free energy surface, the ensemble of initially denatured molecules partition into fast folders (Φ being their fraction) and slow folders.

If the transitions from the CBAs to NBA occur rapidly enough (i.e., within biologically relevant times), then the assistance of chaperonins is not required. The need for chaperonin-assisted folding arises only if the following two conditions are met: (a) The polypeptide chain predominantly misfolds so that the fraction, Φ , of molecules that reach the native conformation directly by a nucleation-collapse mechanism is small. (b) The time scale for transitions from the misfolded structures to the native state becomes comparable to biologically relevant times. Misfolding occurs for polypeptide chains whenever the initial collapse is nonspecific (incorrect nucleation) (55). If these two conditions are satisfied, then the rescue from the misfolded states would require chaperonins. Because the energy landscape can be altered by changing the external conditions (pH, temperature, ionic strength of buffers, and concentration of the polypeptide), it is possible that a polypeptide chain, which would be a two-state folder under certain conditions, becomes a slow folder when the conditions are altered. The combined GroEL-GroES machine can be used to rescue such systems under the nonpermissive conditions.

An important consequence of the rough energy landscape is that, even under nonpermissive conditions, there is a small probability that a certain fraction of molecules will reach the native conformation via a direct pathway within several milliseconds. The fraction of molecules that reach the native conformation by this direct pathway is governed by the partition factor, Φ , that depends on intrinsic factors (amino acid sequence) and external conditions. The description based on the energy landscape perspective is valid for all proteins. For two-state folders,

$\Phi \simeq 1$. The need for chaperonin-mediated folding arises whenever Φ is so small so that appreciable yield of the folded protein is not accumulated on biologically relevant time scale.

Theoretical Considerations

The dynamic process of binding and release of the SP by the chaperonin system is characterized by several time scales. Upon capture by the GroEL ring (Figure 1), the SP experience a hydrophobic surface. Let τ_H be the time in which the SP experiences hydrophobic interactions. After encapsulation, the SP experiences a hydrophilic surface. Let τ_P be the time scale for which the wall is hydrophilic. These two time scales (τ_H and τ_P) may be associated with the two-stage allosteric transitions in the GroEL system (see below). The total cycle time, which is cumulatively associated with the start of capture till relaxation back to the state in which the GroEL can again bind to SP, is approximately $\tau_P + \tau_H$. We assume that all other processes such as binding of nucleotides and GroES and the relaxation to an acceptor state are rapid.

By focusing on these two fundamental time scales, which are most relevant for folding of SPs, we can explore the various limits of the IAM. Recent experiments (38, 52, 74) and computations (3) suggest that the change in the interaction between the SP and GroE system leads to an unfolding of the sequestered protein. This naturally puts the SP on a higher free energy on the landscape. After release from the walls of GroEL into the central cavity, the SP undergoes kinetic partitioning. In light of the time scales noted above, the most productive folding occurs during τ_P . The mere act of capture and providing an effective hydrophobic surface for the duration τ_H is sufficient to enable many proteins to reach a competent conformation (i.e., GroEL can be thought of as a continuous annealing machine) (9). This is in accord with experiments on barnase, which reaches the native state in the presence of GroEL without ATP or GroES (23). However, efficient folding requires a complete system (GroEL/GroES/ATP) that subjects the SP to alternating hydrophilic and hydrophobic surfaces (3, 47, 53). Upon a change in the nature of the interaction between the SP and the interior of the cavity, the SP undergoes kinetic partitioning so that in the first cycle, the fraction of unfolded molecules on the time scale τ_P

$$P_u(t) \simeq \Phi \exp\left(-\frac{\tau_P}{\tau_F}\right) + (1 - \Phi) \exp\left(-\frac{\tau_P}{\tau_S}\right), \quad (1)$$

where τ_F is the folding time for direct (nucleation-collapse) pathway, τ_S is the folding time for transition from misfolded conformations to the native state, and Φ is the partition factor.

There are three scenarios that emerge depending upon the relative values of τ_P , τ_F , and τ_S .

- (i) $\tau_F \ll \tau_S \ll \tau_P$: According to Equation 1, the fraction of unfolded molecules on the time scale τ_P is approximately zero, which implies that

these proteins do not require chaperonins for folding. Such proteins fold spontaneously by an apparent two-state kinetics or by KPM. It is suspected that the majority of proteins in *E. coli* fall in this category (32).

- (ii) $\tau_F \ll \tau_P \ll \tau_S$: This situation pertains to proteins for which Φ is small and τ_S is so long that aggregation prevents spontaneous folding. The conditions under which this occurs are nonpermissive. Using Equation 1, it is easy to show that after n cycles (or iterations) the yield of the native state is (57)

$$\Psi_N = 1 - (1 - \Phi)^n. \quad (2)$$

In obtaining the above equation, we have assumed that Φ is independent of the iteration cycle. Previously, we showed that this scenario describes the folding of Rubisco ($\Phi \approx 0.05$) under nonpermissive conditions (57). We find that for $\Phi \approx 0.05$, 20 cycles are needed to get $\Psi_N = 0.7$. It appears that majority of the SPs that have been used in in vitro studies appear to satisfy this condition.

- (iii) $\tau_F \ll \tau_P \approx \tau_S$: Under these conditions, we find using Equation 1 that the native state yield after n iterations is

$$\Psi_N = 1 - \left(\frac{1 - \Phi}{e} \right)^n, \quad (3)$$

where $\ln e = 1$. Even for proteins with $\Phi = 0.05$, only two iterations are required to get $\Psi_N \simeq 0.9$. We are not aware of any examples that conform to this pattern. However, only a miniscule fraction of *E. coli* proteome has been examined for their interaction with chaperonins.

COMMUNICATION BETWEEN RINGS

Allosteric Transitions

In the previous sections, we showed that the fundamental processes in chaperonin-assisted folding may be understood in terms of the action of a single ring. However, in the course of assisted folding, the two heptameric rings undergo substantial conformational changes that are coupled to ATP binding, to hydrolysis, and to interactions with the cochaperonin GroES (47, 68, 69). The transitions within a ring and inter-ring communications are essential for efficient operation of the chaperonin machinery. In the double ring there are 14 ATP binding sites. The binding of ATP and its hydrolysis exhibit positive cooperativity within each ring and negative cooperativity between rings (71). The positive cooperativity is reflected in the relatively low ATP concentration ($\leq 100 \mu\text{M}$) needed for transitions in the one ring from a low-affinity (with respect to ATP binding) *T* state to a high-affinity *R* state. Conversely, the transition in the other ring from a low-affinity

state to a high-affinity state requires much higher concentration of ATP, thus explaining the interring negative cooperativity. These allosteric properties and the interactions with GroES are believed to play a pivotal role in the rescue of misfolded SPs.

Yifrach & Horovitz used extensive experiments and mathematical models to understand quantitatively the complicated allosteric transitions in the GroEL particle (71). By systematically examining the ATPase activity in the wild type and mutant, it has been shown that GroEL exhibits nested cooperativity (i.e., there are two levels of allostery). In the first level there is a cooperative transition, $TT \longleftrightarrow TR$, where following the MWC terminology, T is the tense state (low affinity for binding ATP) and R is the relaxed state (high affinity for ATP). Conversely, the T state has a high affinity for binding SP, whereas the R state has lower affinity for SP. The second level of allostery involves the transitions between TT , TR , and RR states, which are best described as a series of sequential steps thus conforming to the Koshland-Nemethy-Filmer (30) model. According to the nested cooperativity model (71), the fractional binding of ATP (saturation curve) is determined by two equilibrium constants, $L_1 = [TR]/[TT]$ and $L_2 = [TR]/[RR]$. The inter-ring negative cooperativity implies $L_2 \ll L_1$. This model quantitatively describes the two-step allosteric transitions of the GroEL rings. Two factors determine the values of L_1 and L_2 . ATP binding increases L_1 and decreases L_2 . Conversely, SP decreases L_1 and increases L_2 (70). Because the efficiency of the chaperonin system depends on the rates of the allosteric transitions, it follows that the equilibrium constants L_1 and L_2 must determine the course of assisted folding in the absence of GroES.

The crystal structures of GroEL and $GroEL \bullet GroES \bullet ADP_7$ have been determined so that the conformations of the T (4) and R'' (68) states are known at atomic resolution. These structures and those derived from cryo-EM micrographs (66) of the wild-type GroEL and a mutant (R197A) have revealed the nature of the rigid body motions in the $T \longleftrightarrow R$ and $R \longleftrightarrow R'$ transitions. From the perspective of assisted folding, it is necessary to understand the dynamics of the transitions during the various stages of the chaperonin cycle. Recent molecular dynamics simulations (34, 35), based on normal mode analysis of individual subunit of GroEL and a model multiunit construct, are beginning to provide the plausible molecular events in the allosteric transitions in GroEL. To a large extent, these simulations reinforce the experimental findings that the intraring transitions are concerted (68). The excluded volume interactions between the apical domain of one subunit in the R state with its neighbor in the T state are the major contributor to concertedness (35). The normal mode analysis also showed that the interactions between the equatorial domains are the source of negative cooperativity between the rings. In the process of $T \rightarrow R$ (or R') transition, the equatorial domain of the *cis* (upper) ring pushes down on the lower ring causing a reverse tilt of the equatorial domain in the *trans* (lower) ring (68). These observations are in accord with the crystal structure of the R'' state (68).

Allosteric Transitions and SP Folding

An important issue that is not fully understood pertains to the coupling between the allosteric transitions the GroEL particle undergoes and folding of the SP. This question is difficult to sort out using currently available experimental probes, especially when the participation of the cofactor GroES is taken into account. To illustrate the issues that arise, we again consider the hemicycle (Figure 1). The allosteric transitions are thought to take place in two steps: $T \longleftrightarrow R$ occurs upon nucleotide binding. Let the rate for this transition be $k_{T \rightarrow R}$. Fluorescent emission studies in the mutant Phe44 \rightarrow Trp in GroEL show that in the presence of ATP $k_{T \rightarrow R} > 100 \text{ s}^{-1}$ (72). The surface of the cavity is less hydrophobic in the R state than in the T state, accounting for the lower affinity of SP for the R state. Therefore it is possible that this conformational change alone is sufficient for inducing folding of some SPs that would make GroEL a continuous annealing machine. For such SPs, the rates of folding can either increase or decrease in the presence of GroEL depending on the strength of interaction with the chaperonin (5, 28, 42, 55). It is worth emphasizing that even in this situation the motion of the subunits leads to work on the SP, implying that the passive Anfinsen cage model would be inapplicable.

The second step involves a $R \longleftrightarrow R'$ transition that is mediated by interactions with the GroES particle. We denote the rate of this transition, which is believed to be diffusion limited, as $k_{R \rightarrow R'}$. After the second stage the encapsulated SP is largely subject to hydrophilic interactions. Concomitant with ATP hydrolysis, $R' \longleftrightarrow R''$ transition occurs at a rate $k_{R' \rightarrow R''}$. This is followed by binding of ATP to the *trans* ring, which serves as a signal for the release of all of the ligands from the *cis* ring restoring that ring to the T state. The rate for the discharge and release step is $k_{R' \rightarrow T}$.

The productive folding time is approximately $\tau_P \approx k_{R \rightarrow R'}^{-1} + k_{R' \rightarrow R''}^{-1}$. A quantitative understanding of the coupling between allostery in GroEL and SP folding requires measurements of the five transition rates implied by the hemicycle (Figure 1). This analysis underscores the importance of the dynamics connecting the T , R , R' , and R'' states in the rescue of the SPs. Our description also suggests that a quantitative study of the coupling between SP and allostery is complicated because of the interplay of several time scales ($k_{R \rightarrow T}^{-1}$, $k_{T \rightarrow R}^{-1}$, $k_{R \rightarrow R'}^{-1}$, $k_{R' \rightarrow R''}^{-1}$, $k_{R'' \rightarrow T}^{-1}$, τ_F , and τ_S). In the absence of GroES, one need only consider $k_{T \rightarrow R}^{-1}$, $k_{R \rightarrow T}^{-1}$, τ_F , and τ_S .

Recently the link between assisted folding rates and the allosteric transition for two SPs has been studied (73). The assisted folding of dihydrofolate reductase (DHFR) requires only GroEL and ATP. That is to say it involves the times $k_{T \rightarrow R}$, τ_F , and τ_S . In this case the only relevant allosteric transition is delineated by a single equilibrium constant, L_1 , describing the $T \longleftrightarrow R$. The folding rate of DHFR decreases as the extent of intraring cooperativity increases as measured by the Hill coefficient, n_H (73). The numerical value of n_H is a measure of the extent of

inter-ring cooperativity in the $T \longleftrightarrow R$ transition. Thus, there is an inverse correlation between the extent of cooperativity and SP refolding rates of DHFR. This result was anticipated in a lattice simulation of folding in a dynamic cavity (3). The chaperonin GroEL was modeled as a cavity whose walls can undergo transitions from hydrophobic lining to a hydrophilic surface. This mimics the changes that the SPs experience as GroEL undergoes the $T \longleftrightarrow R$ transition. The effect of cycling between the extreme environments was simulated as a function of $\frac{\tau_H}{\tau_P}$. This ratio is, approximately, the allosteric equilibrium constant in the experiments (73), and hence is related to n_H . In accord with experiments on DHFR, folding rates and the ratio $\frac{\tau_H}{\tau_P}$ showed an inverse correlation. Because each cycling leads to unfolding, it follows that if the frequency of the unfoldase activity (controlled by n_H) of GroEL is increased, then the efficiency of assisted folding would increase as well. The computational (3) and the experimental (73) study established, for the first time, in a model system without the cochaperonin GroES the relationship between the equilibrium allosteric transition and the folding rates of the SPs.

The reactivation of malate dehydrogenase (MDH) requires the complete chaperonin system. Our analysis suggests that the link between the SP folding rate and the allosteric transition of GroEL is complex. Because the transition rates between the states that GroEL traverses in the hemicycle can be altered by external conditions, the effect of GroES on the SP folding rate depends on the experimental conditions. In the experiments (73), the refolding rate of MDH was insensitive to the extent of negative cooperativity observed in various GroEL mutants when GroES was added. It is not clear if this is because MDH under the experimental conditions folds in the absence of GroEL. Quantitative study of the relationship between the folding rates of SPs and the extent of positive and negative cooperativity in GroEL requires additional experiments.

The major difficulty in linking the SP folding rate and the equilibrium allosteric transitions of GroEL arises because the system is far from equilibrium in the presence of GroES and ATP. In particular, upon addition of GroES, the system is committed to completing the various irreversible steps in the hemicycle (Figure 1). To a first approximation, τ_P and τ_H determine the SP folding rate. Although these fundamental time constants of the cycle are linked to the allosteric transitions that GroEL undergoes, we do not expect them to be directly related to the equilibrium constants L_1 and L_2 .

SINGLE MOLECULE MEASUREMENTS

In the discussions so far, we have assumed that for a given external condition, single unique values specify the fundamental time constants in the hemicycle. This simplification allows us to discuss the mechanisms of chaperonin action without involving the potential heterogeneities in the interactions between GroEL, GroES, and SP. However, single molecule studies are beginning to show that considerable

variations in the interactions between components of the chaperonin system are possible. Such variations suggest that in this driven system the most probable values of interaction free energies and time constants need not be close to the average values measured in bulk experiments.

A recent experiment, using a small cantilever atomic force microscope, provided direct evidence for large variations in the dissociation constant of GroES from the GroES-GroEL complex. Small cantilever AFMs were used to image GroEL immobilized on a mica surface. As the sample is scanned, a rise in the step indicates that a molecule is adsorbed onto the surface. Upon adding GroES and ATP, images of the sample were taken every 100 msec over a period of about 120 seconds. The difference in the step heights between the two samples indicates whether a complex exists or not. By scanning across the same GroEL molecule over a time period, a histogram of the complex lifetimes can be obtained. It was found that the distribution of the lifetime of the complex (or the dissociation rate of GroES) was extremely broad. Qualitatively, the distribution can be described by $P_{lt}(t) \sim t \exp(-\frac{t}{\tau_0})$ with $\tau_0 \approx 3.5$ s. The average lifetime of 7 s is different from the most likely value of 5 s. More important, the fluctuations in the time scale are on the order of 7 s, which underscores the considerable dispersion. The large dispersion suggests that the interaction between the GroES and GroEL is varied so that each association produces a complex with somewhat differing structure. If this interpretation is correct, it would imply that, in a typical pulling experiment using AFM, there should be large dispersion in the forces holding GroES and GroEL.

An earlier single molecule AFM experiment (62) showed that there is a large heterogeneity in the interactions between GroEL and SPs. This is vividly illustrated in the measured distribution of threshold forces between SPs and GroEL for mutants of citrate synthase and β -lactamase. Based on biochemical studies of GroEL interactions with SPs and their effect on the $T \longleftrightarrow R$ transition (70), we expect that the AFM experiments should lead to the following results: (a) The threshold forces should be less when the SP is in the native state than when it is unfolded. (b) Addition of ATP, which leads to the $T \longleftrightarrow R$ transition, should lead to a decrease in the forces between GroEL and the SPs. (c) As the molecular weight increases we expect that the unfolded SP would interact with more subunits of GroEL. This suggests that the interaction energies with GroEL should increase as the molecular weight of the SP increases. The force distribution can be used to estimate the free energy of interaction, ΔG , between the SP in the denatured state and the GroEL. We estimate ΔG in reference to binding of the SP in the native state. We can write $\Delta G \approx (F_D - F_N)\Delta x$, where $\Delta x = A'B' - AB$ (see Figure 2) is the subunit displacement in the $T \longleftrightarrow R$ transition, F_D is the mean force of interaction between the SP and GroEL when SP is in the denatured state, and F_N is the corresponding value when the SP is in the native conformation. For β -lactamase, the measured values of F_D and F_N are 340pN and 250pN, respectively. If we assume that $\Delta x \approx 0.2$ nm, we get $\Delta G \approx 3$ kcal/mole. A similar calculation using $F_D = 770$ pN and $F_N = 350$ pN for citrate synthase gives $\Delta G \approx 12$ kcal/mole.

We should caution that there is considerable dispersion in the forces. For citrate synthase the dispersion is approximately 200pN. Thus, the dispersion in ΔG can be as large as 6 kcal/mole. Thus, AFM experiments can be used to obtain the interaction free energies between protein complexes.

The general expectations sketched above are borne out in the AFM experiments (62). However, there were two surprises: (a) The distribution of forces showed considerable dispersion for the two SPs, which indicated that there is structural diversity in the GroEL-SP complex. The dispersion in the force distribution was considerably greater when the SP is in the unfolded state. Assuming that the structural fluctuations of GroEL were minimal, we conclude that the dispersion arose because of the structural inhomogeneity of the SP. (b) The increase in interaction energies with increasing molecular weight of SP is consistent with the notion that larger SPs need to be pinned at more subunits than smaller ones. This argument would also suggest that fluctuations in the SP structure should decrease with increasing molecular weight. This would give rise to smaller dispersions in the force distributions for higher molecular weight SPs. The AFM experiments show the opposite trend. The dispersion in forces in citrate synthase is larger than in β -lactamase. It would be interesting to extend these studies to other SPs.

An estimate of the stretching force imparted to the SP can be made using dimensional analysis. Assume that initially the SP interacts only with two adjacent subunits *A* and *B* (Figure 2) when GroEL is in the *T* state. After the $T \longleftrightarrow R$ transition, these subunits move apart by a distance Δx (Figure 2). The value of Δx depends on the location of the initial SP binding sites. The loss of interaction between the binding sites and the SP sets the scale for the force that can be imparted to the SP. From dimensional analysis it follows that the stretching force $F_{STR} \approx k_B T / \Delta x$. If $\Delta x \approx 0.2$ nm, then $F_{STR} \approx 20$ pN. This force would be sufficient to unfold, at least partially, many single domain proteins (20) provided that the pulling speed, *v*, is small. In the case of GroEL, $v \approx \Delta x k_{T \rightarrow R} \approx 2 \times 10^{-6}$ $\mu\text{m/s}$. By comparison the typical pulling speed in AFM experiments involving titin is 0.1 $\mu\text{m/s}$ (20). At this higher pulling speed, about 150pN is required to globally unfold the immunoglobulin in domains of titin. Considering that *v* in GroEL is nearly five orders of magnitude slower the estimate of F_{STR} is physically reasonable. The dimensional analysis also suggests that F_{STR} will be smaller if the SP interacts with subunits that are further apart. This prediction can be verified by AFM experiments involving mutations in the GroEL subunits that prevent it from being a binding site for the SP (13).

We have proposed that the unfolding of the SP occurs by a force that is transmitted to it by the twisting motion of the apical domains that accompanies the two concerted allosteric transitions ($T \longleftrightarrow R$ and $R \longleftrightarrow R'$). The efficient transmission of this unfolding force requires the dense inertial mass, which is provided by the equatorial plate. This structural feature may be an important element in the function of other unfolding machines.

ACKNOWLEDGMENTS

We thank A Horovitz for helpful discussions. This work is supported by NSF Grant CHE-99-75150.

Visit the Annual Reviews home page at www.AnnualReviews.org

LITERATURE CITED

1. Aoki K, Motojima F, Taguchi H, Yomo T, Yoshida M. 2000. GroEL binds artificial proteins with random sequences. *J. Biol. Chem.* 275:13755–58
2. Aoki K, Taguchi H, Shindo Y, Yoshida M, Ogasahara K, et al. 1995. Calorimetric observation of a groel-protein binding reaction with little contribution of hydrophobic interaction. *J. Biol. Chem.* 272:32158–62
3. Betancourt MR, Thirumalai D. 1999. Exploring the kinetic requirements for enhancement of protein folding rates in the GroEL cavity. *J. Mol. Biol.* 287:627–44
4. Braig K, Otwinowski Z, Hedge R, Boisvert DC, Joachimiak A, et al. 1994. The crystal structure of the bacterial chaperonin at 2.8Å. *Nature* 371:578–86
5. Chan HS, Dill KA. 1996. A simple model of chaperonin-mediated protein folding. *Protein: Struct. Funct. Genet.* 24:345–51
6. Chatellier J, Buckle AM, Fersht AR. 1999. GroEL recognizes sequential and nonsequential linear structural motifs compatible with extended β -strands and α -helices. *J. Mol. Biol.* 292:163–72
7. Chen L, Sigler PB. 1999. The crystal structure of a GroEL/peptide complex: plasticity as a basis for substrate diversity. *Cell* 99:757–68
8. Clark AC, Frieden C. 1999. The chaperonin GroEL binds to late-folding nonnative conformations present in native *Escherichia coli* and murine dihydrofolate reductases. *J. Mol. Biol.* 285:1777–88
- 8a. Cliff MJ, Kad NM, Hay N, Luno PA, Webb MR, et al. 1999. A kinetic study of the nucleotide-induced allosteric transitions of GroEL. *J. Mol. Biol.* 293:667–84
9. Corrales FJ, Fersht AR. 1996. Toward a mechanism of GroEL-GroES chaperone activity: an ATPase-gated and pulsed folding and annealing cage. *Proc. Natl. Acad. Sci. USA* 93:4509–12
10. Dill KA, Chan HS. 1997. From Levinthal to pathways to funnels. *Nat. Struct. Biol.* 4:10–19
11. Eaton WA, Munoz V, Henry ER, Hofrichter J. 1999. Kinetics and dynamics of loops, α -helices, β -hairpin and fast folding proteins. *Acc. Chem. Res.* 31:745–53
12. Ewalt LL, Hendrick JP, Houry WA, Hartl FU. 1997. In vivo observation of polypeptide flux through the bacterial chaperonin system. *Cell* 90:491–500
13. Farr GW, Furtak K, Rowland MB, Ranson NA, Saibil HR, et al. 2000. Multivalent binding of non-native substrate proteins by the chaperonin GroEL. *Cell* 100:561–73
14. Fayet O, Louarn JM, Georgopoulos C. 1986. Suppression of the *Escherichia coli* dnaa46 mutation by amplification of the groes and groel genes. *Mol. Gen. Genet.* 202:435–45
15. Federov AN, Baldwin TO. 1997. GroEL modulates kinetic partitioning of folding intermediates between alternative states to maximize the yield of biological active protein. *J. Mol. Biol.* 268:712–23
16. Fenton WA, Horwich AL. 1997. GroEL-mediated protein folding. *Protein Sci.* 6:743–60
17. Fenton WA, Kashi Y, Furtak K, Horwich AL. 1994. Residues in chaperonin groel required for polypeptide binding and release. *Nature* 371:614–19
18. Fersht AR. 1997. Nucleation mechanisms

- in protein folding. *Curr. Opin. Struct. Biol.* 7:3–9
19. Fisher MT. 1994. The effect of GroES on the groel-dependent assembly of dodecameric glutamine synthetase in the presence of ATP and ADP. *J. Biol. Chem.* 269:13629–36
 20. Fisher TE, Marszalek PE, Fernandez JM. 2000. Stretching single molecules into novel conformations using the atomic force microscope. *Nat. Struct. Biol.* 9:719–24
 21. Gordon CL, Sather SK, Casjens S, King J. 1994. Selective in vivo rescue by groel/es of thermolabile folding intermediates to phage p22 structural proteins. *J. Biol. Chem.* 269:27941–51
 22. Grallert H, Rutkat K, Buchner J. 2000. Limits of protein folding inside GroE complexes. *J. Biol. Chem.* 275:20424–30
 23. Gray TE, Fersht AR. 1993. Refolding of barnase in the presence of GroE. *J. Mol. Biol.* 232:1197–1207
 24. Gulukota K, Wolynes PG. 1994. Statistical mechanics of kinetic proof reading in protein folding *in vivo*. *Proc. Natl. Acad. Sci. USA* 91:9292–96
 25. Guo Z, Thirumalai D. 1995. Protein folding: nucleation mechanism, time scales and pathways. *Biopolymers* 36:83–102
 26. Horovitz A, Yifrach O. 2000. On the relationship between the Hill coefficients for steady-state and transient kinetic data: a criterion for concerted transitions in allosteric proteins. *Bull. Math. Biol.* 62:241–46
 27. Houry WA, Fishman D, Eckerskom C, Lottspeich F, Hartl FU. 1999. Identification of textitin vivo substrates of the chaperonin GroEL. *Nature* 402:147–54
 - 27a. Inbar E, Horovitz A. 1997. GroES promotes the T to R transition of the GroEL ring distal to GroES in the GroEL-GroES complex. *Biochemistry* 36:12276–81
 28. Itzhaki LS, Otzen DE, Fersht AR. 1995. Nature and consequences of GroEL-protein interactions. *Biochemistry* 34:14581–87
 29. Katsumata K, Okazaki A, Tsurpa GP, Kuwajima K. 1996. Dominant forces in the recognition of a transient folding intermediate of alpha-lactalbumin by GroEL. *J. Mol. Biol.* 264:643–49
 30. Koshland DE, Nemethy G, Filmer D. 1966. Comparison of experimental binding data and theoretical models in proteins containing subunits. *Biochemistry* 5:365–85
 31. Lin Z, Schwartz FP, Eisenstein E. 1995. The hydrophobic nature of GroEL-substrate binding. *J. Biol. Chem.* 270:1011–14
 32. Lorimer GH. 1996. A quantitative assessment of the role of the chaperonin proteins in protein folding *in vivo*. *FASEB J.* 10:5–9
 33. Lorimer GH. 1997. Folding with a two-stroke motor. *Nature* 388:720–23
 34. Ma J, Karplus MK. 1998. The allosteric mechanism of the chaperonin GroEL: a dynamic analysis. *Proc. Natl. Acad. Sci. USA* 95:8502–7
 35. Ma J, Sigler PB, Xu ZH, Karplus M. 2000. A dynamic model for allosteric mechanism for GroEL. *J. Mol. Biol.* 302:303–13
 36. Monod J, Wyman J, Changeaux JP. 1965. On the nature of allosteric interactions: a plausible model. *J. Mol. Biol.* 12:88–118
 37. Munoz V, Thompson PA, Hofrichter J, Eaton WA. 1997. Folding dynamics and mechanism of β -hairpin formation. *Nature* 390:196–99
 38. Nieba-Axmann SE, Ottinger M, Wuthrich K, Pluckthun A. 1997. Multiple cycles of global unfolding of GroEL-bound cyclophilin A evidenced by NMR. *J. Mol. Biol.* 271:803–18
 39. Nielsen KL, Cowan NJ. 1998. A single ring is sufficient for productive chaperonin-mediated folding *in vivo*. *Mol. Cell* 2:93–99
 40. Nielsen KL, McLennan N, Masters M,

- Cowan NJ. 1999. A single-ring mitochondrial chaperonin (Hsp60-Hsp10) can substitute for GroEL-GroES in vivo. *J. Bacteriol.* 181:5871–75
41. Onuchic JN, Luthey-Schulten Z, Wolynes PG. 1997. Theory of protein folding: the energy landscape perspective. *Annu. Rev. Phys. Chem.* 48:545–600
 42. Orland H, Thirumalai D. 1997. A kinetic model for chaperonin assisted protein folding. *J. Phys.* 7:553–60
 43. Pack CG, Aoki K, Taguchi H, Yoshida M, Kinjo M, Tamura M. 2000. Effect of electrostatic interaction on the binding of charged substrate to groel studied by highly sensitive fluorescence correlation spectroscopy. *Biochem. Biophys. Res. Commun.* 267:300–4
 44. Perrett S, Zahn R, Stenberg G, Fersht AR. 1997. Importance of electrostatic interactions in the rapid binding of polypeptides to GroEL. *J. Mol. Biol.* 269:892–901
 45. Richardson A, Landry SJ, Georgopolulos C. 1998. The ins and outs of a molecular chaperone machine. *Trends Biochem. Sci.* 23:138–43
 46. Richarme G, Kohiyama M. 1994. Amino acid specificity of the *Escherichia coli* chaperone GroEL (heat shock protein 60). *J. Biol. Chem.* 269:7095–98
 47. Rye HS, Burston SG, Fenton WA, Beechem JM, Xu Z, et al. 1997. Distinct actions of *cis* and *trans* ATP within the double ring of the chaperonin GroEL. *Nature* 388:792–98
 48. Rye HS, Roseman AM, Chen S, Furtak K, Fenton WA, et al. 1999. GroEL-GroES cycling: ATP and non-native polypeptide direct alternation of folding-active rings. *Cell* 97:325–38
 49. Saibil H. 2000. Molecular chaperones: containers and surfaces for folding, stabilizing or unfolding proteins. *Curr. Opin. Struct. Biol.* 10:251–58
 50. Sakikawa C, Taguchi H, Makino Y, Yoshida M. 1999. On the maximum size of proteins to stay and fold in the cavity of GroEL underneath GroES. *J. Biol. Chem.* 274:21251–56
 51. Shastry MC, Roder H. 1999. Evidence for barrier-limited protein folding on the microsecond time scale. *Nat. Struct. Biol.* 5:385–92
 52. Shtilerman M, Lorimer GH, Englander SW. 1999. Chaperonin function: folding by forced unfolding. *Science* 284:822–25
 53. Sigler PB, Xu Z, Rye HS, Burston SG, Fenton WA, Horwich AL. 1998. Structure and function GroEL-mediated protein folding. *Annu. Rev. Biochem.* 67:581–608
 54. Thirumalai D. 1994. Theoretical and perspectives on *in vitro* and *in vivo* folding. In *Statistical Mechanics, Protein Structure, and Protein-Substrate Interactions*, ed. S Doniach, pp. 115–34. New York: Plenum
 55. Thirumalai D. 1995. From minimal models to real proteins: time scales for protein folding kinetics. *J. Phys.* 5:1457–67
 56. Thirumalai D, Klimov DK, Woodson SA. 1997. Kinetic partitioning mechanism as a unifying theme in the folding of biomolecules. *Theor. Chem. Acc.* 1:23–30
 57. Todd MJ, Lorimer GH, Thirumalai D. 1996. Chaperonin-facilitated protein folding: optimization of rate and yield by an iterative mechanism. *Proc. Natl. Acad. Sci. USA* 93:4030–35
 58. Todd MJ, Viitanen PV, Lorimer GH. 1994. Dynamics of the chaperonin ATPase cycle: implications for facilitated protein folding. *Science* 256:659–66
 59. Van Dyk TK, Gatenby AA, LaRossa RA. 1989. Demonstration by genetic suppression of interaction of groe products with many proteins. *Nature* 342:451–53
 60. Viani MB, Pietrasanta LI, Thompson JB, Chand A, Gebeshuber IC, et al. 2000. Probing protein-protein interactions in real time. *Nat. Struct. Biol.* 7:644–47
 61. Viitaen PV, Gatenby AA, Lorimer GH. 1992. Purified chaperonin 60 (GroEL) interacts with the non-native states of a

- multitude of *Escherichia coli* proteins. *Protein Sci.* 1:363–69
62. Vinckier A, Gervasoni P, Zaugg F, Ziegler U, Lidner P, et al. 1998. Atomic force microscopy detects changes in the interaction forces between GroEL and substrate proteins. *Biophys. J.* 74:3256–63
63. Walter S, Lorimer GH, Schmid FX. 1996. A thermodynamic coupling mechanism for GroEL-mediated unfolding. *Proc. Natl. Acad. Sci. USA* 93:9425–30
64. Weissman JS, Kashi Y, Fenton WA, Horowich AL. 1994. GroEL-mediated protein folding proceeds by multiple rounds of binding and release of non-native forms. *Cell* 78:693–702
65. Weissman JS, Rye HS, Fenton WA, Beechem JM, Horowich AL. 1996. Characterization of the active intermediate of a GroEL-GroES mediated protein folding. *Cell* 84:481–90
66. White HE, Chen S, Roseman AM, Yifrach O, Horovitz A, Saibil H. 1997. Structural basis of allosteric changes in the GroEL mutant Arg197 → Ala. *Nat. Struct. Biol.* 4:690–94
67. Wilkins DK, Grimshaw SB, Receveur V, Dobson CM, Jones JA, Smith JA. 1999. Hydrodynamic radii of native and denatured proteins measured by pulse field gradient NMR techniques. *Biochemistry* 38:16424–31
68. Xu Z, Horowich A, Sigler PB. 1997. The crystal structure of the asymmetric GroEL-GroES-(ADP)₇ chaperonin complex. *Nature* 388:741–50
69. Xu Z, Sigler PB. 1999. GroEL/GroES: structure and function of a two-stroke folding machine. *J. Struct. Biol.* 124:129–41
70. Yifrach O, Horovitz A. 1996. Allosteric control by ATP of non-native protein binding to GroEL. *J. Mol. Biol.* 255:356–61
71. Yifrach O, Horovitz A. 1995. Nested cooperativity in the ATPase activity of the oligomeric chaperonin GroEL. *Biochemistry* 35:5303–8
72. Yifrach O, Horovitz A. 1998. Transient kinetic analysis of adenosine 5'-triphosphate binding-induced conformational changes in the allosteric GroEL. *Biochemistry* 37:7083–88
73. Yifrach O, Horovitz A. 2000. Coupling between protein folding and allostery in the GroE chaperonin system. *Proc. Natl. Acad. Sci. USA* 97:1521–24
74. Zahn R, Perrett S, Stenberg G, Fersht AR. 1996. Catalysis of amide proton exchange by the molecular chaperones GroEL and SecB. *Science* 271:642–45



CONTENTS

HYDROGEN BONDING, BASE STACKING, AND STERIC EFFECTS IN DNA REPLICATION, <i>Eric T. Kool</i>	1
STRUCTURES AND PROTON-PUMPING STRATEGIES OF MITOCHONDRIAL RESPIRATORY ENZYMES, <i>Brian E. Schultz, Sunney I. Chan</i>	23
MASS SPECTROMETRY AS A TOOL FOR PROTEIN CRYSTALLOGRAPHY, <i>Steven L. Cohen, Brian T. Chait</i>	67
A STRUCTURAL VIEW OF Cre-loxP SITE-SPECIFIC RECOMBINATION, <i>Gregory D. Van Duyne</i>	87
PROBING THE RELATION BETWEEN FORCE--LIFETIME--AND CHEMISTRY IN SINGLE MOLECULAR BONDS, <i>Evan Evans</i>	105
NMR PROBES OF MOLECULAR DYNAMICS: Overview and Comparison with Other Techniques, <i>Arthur G. Palmer III</i>	129
STRUCTURE OF PROTEINS INVOLVED IN SYNAPTIC VESICLE FUSION IN NEURONS, <i>Axel T. Brunger</i>	157
AB INITIO PROTEIN STRUCTURE PREDICTION: Progress and Prospects, <i>Richard Bonneau, David Baker</i>	173
STRUCTURAL RELATIONSHIPS AMONG REGULATED AND UNREGULATED PHOSPHORYLASES, <i>Jenny L. Buchbinder, Virginia L. Rath, Robert J. Fletterick</i>	191
BIOMOLECULAR SIMULATIONS: Recent Developments in Force Fields, Simulations of Enzyme Catalysis, Protein-Ligand, Protein-Protein, and Protein-Nucleic Acid Noncovalent Interactions, <i>Wei Wang, Oreola Donini, Carolina M. Reyes, Peter A. Kollman</i>	211
CHAPERONIN-MEDIATED PROTEIN FOLDING, <i>D. Thirumalai, George H. Lorimer</i>	245
INTERPRETING THE EFFECTS OF SMALL UNCHARGED SOLUTES ON PROTEIN-FOLDING EQUILIBRIA, <i>Paula R. Davis- Searles, Aleister J. Saunders, Dorothy A. Erie, Donald J. Winzor, Gary J. Pielak</i>	271
PHOTOSYSTEM II: The Solid Structural Era, <i>Kyong-Hi Rhee</i>	307
BINDING OF LIGANDS AND ACTIVATION OF TRANSCRIPTION BY NUCLEAR RECEPTORS, <i>Anke C. U. Steinmetz, Jean-Paul Renaud, Dino Moras</i>	329
PROTEIN FOLDING THEORY: From Lattice to All-Atom Models, <i>Leonid Mirny, Eugene Shakhnovich</i>	361
STRUCTURAL INSIGHTS INTO MICROTUBULE FUNCTION, <i>Eva Nogales</i>	397
PROPERTIES AND BIOLOGICAL ACTIVITIES OF THIOREDOXINS, <i>Garth Powis, William R Montfort</i>	421
RIBOZYME STRUCTURES AND MECHANISMS, <i>Elizabeth A. Doherty, Jennifer A. Doudna</i>	457